Transcriptome Analysis Reveals Dynamic Changes of Inflammation and Stress Responses during Different Infected Stages with *Burkholderia pseudomallei*

Chenglong Rao(Former Corresponding Author)
Department of Clinical Microbiology and Immunology, College of Pharmacy and Medical Laboratory, Army Medical University (Third Military Medical University), Chongqing, China. https://orcid.org/0000-0001-6110-2332

Chan Mao
Department of Clinical Microbiology and Immunology, College of Pharmacy and Medical Laboratory, Army Medical University (Third Military Medical University),Chongqing, China.

Yupei Xia
Department of Clinical Microbiology and Immunology, College of Pharmacy and Medical Laboratory, Army Medical University (Third Military Medical University), Chongqing, China.

Meijuan Zhang
Department of Clinical Microbiology and Immunology, College of Pharmcy and Medical Laboratory, Army Medical University (Third Military Medical University), Chongqing, China.

Zhiqiang Hu
Department of Clinical Microbiology and Immunology, College of Pharmacy and Medical Laboratory, Army Medical University (Third Military Medical University), Chongqing, China.

Siqi Yuan
Department of Clinical Microbiology and Immunology, College of Pharmacy and Medical Laboratory, Army Medical University (Third Military Medical University), Chongqing, China.

Yu Zhang
Department of Clinical Microbiology and Immunology, College of Pharmacy and Medical Laboratory, Army Medical University (Third Military Medical University). Chongqing, China.

Jingmin Yan
Department of Clinical Microbiology and Immunology, College of Pharmacy and Medical Laboratory, Army Medical University (Third Military Medical University), Chongqing, China.

Ling Deng
Department of Clinical Microbiology and Immunology, College of Pharmacy and Medical Laboratory, Army Medical University (Third Military Medical University), Chongqing, China.

Xuhu Mao

Department of Clinical Microbiology and Immunology, College of Pharmacy and Medical Laboratory, Army Medical University (Third Military Medical University), Chongqing, China.

Qian Li

Department of Clinical Microbiology and Immunology, College of Pharmacy and Medical Laboratory,Army Medical University (Third Military Medical University), Chongqing, China.

Yaling Liao(New Corresponding Author) (**450187169@qq.com**)

https://orcid.org/0000-0001-6443-9520

Research article

Keywords: Burkholderia pseudomallei, Multinucleated Giant Cells (MGCs), Transcriptomics, Inflammation, Stress response

Posted Date: January 31st, 2020

DOI: https://doi.org/10.21203/rs.2.22365/v1

Version of Record: A version of this preprint was published at Frontiers in Genetics on December 8th, 2020. See the published version at https://doi.org/10.3389/fgene.2020.585203.

Abstract

Background: *Burkholderia pseudomallei* causes melioidosis and usually affects patients' lungs, its persistent infection promotes the fusion of host cells, leading to the formation of multinucleated giant cells (MGCs) at the late infected stage. In this study, the global transcriptomic responses of *B. pseudomallei* infection of a human lung epithelial A549 cell model with different infected stages were investigated by means of microarray analysis to further elucidate the host cellular factors involved in the occurrence and development of the event. Results: A set of 35 common differential expression genes (DEGs) in EI and LI on the mRNA level applying a cut-off level of 1.5-fold change and a p-value < 0.05 were observed. Microarray data were further verified by Real-Time quantitative PCR (RT-qPCR). GO classification and pathway enrichment analysis revealed these DEGs mainly involved in inflammatory response related processes, such as cellular response to tumor necrosis factor, cellular response to lipopolysaccharide, positive regulation of NF-κB transcription factor activity. p-eIF2α, ATF4,NF-κB2(p52) and IL-1β were next selected to be validated by western bloting, which indicated *B. pseudomallei* could activate the eIF2α-ATF4 axis and NF-κB2 pathway in A549 cells. Conclusion: Our data shed light on the transcriptome dynamics of A549 cells which persistently infected with *B. pseudomallei* and suggested that the formation of MGCs may be a means for *B. pseudomallei* to manipulate the host's inflammation and stress response to adapt to intracellular life.

1 Background

Melioidosis is a potentially fatal infectious disease in tropical and subtropical countries worldwide caused by the gram-negative Burkholderia pseudomallei [1]. Humans or animals usually acquire this disease through broken skin, inhalation or ingestion of the pathogen [2]. It is estimated that there are approximately 165,000 cases of human melioidosis each year worldwide and approximately 89,000 deaths (~ 54%) [3]. And with the continuous development of economy and trade, especially the fast development of tourism globalization, the epidemic areas are expanding [1, 3, 4]. In addition, there is no licensed vaccine for the prevention of disease [5]. Therefore, it is urgent to take measures to the disease, and understanding of the intracellular lifestyle by which B. pseudomallei establishes infection will be necessary for the development of approaches to disease control.

B. pseudomallei can adhere to and invade various types of mammalian cells, especially human lung epithelial cells, which are particularly prone to exposure after inhalation [6]. As a facultative intracellular pathogen, B. pseudomallei has a unique intracellular lifestyle in host cells. Escaping from the endocytic vacuole into the cytosol is one characteristic feature during the early stage of infection. It has been reported that B. pseudomallei can escape into the cytoplasm by inducing rearrangement of host actin cytoskeleton and with the help of its type III secretion system (T3SS) effector proteins, such as BopE and BopA [7–9]. Our team previous research found that B. pseudomallei could evade autophagy by 3 novel miRNAs of MIR4458, MIR4667-5p, and MIR4668-5p targeted regulation of ATG10 in A549 cells [10]. Macrophages could up-regulate Rab32 GTPase through reducing miR-30b/30c to accelerate B.

pseudomallei-containing phagosomes maturation [11]. However, B. pseudomallei can escape from Rab32-positive phagosomes into the cytoplasm.

Multinucleated giant cells (MGCs) formation is another important characteristic feature of host cell in the late stage of infection of B. pseudomallei. The persistent infection of B. pseudomallei promotes the fusion of an infected mononuclear cell with one or more adjacent cells leading to the formation of MGCs [12, 13]. The MGCs have also been observed in vivo in autopsy lung tissues of patients with melioidosis and the lung of C57BL/6 mice infected with a low dose of B. pseudomallei [14, 15]. Now, the mechanism for the MGCs formation is still unknown. It is reported that type VI secretion system (T6SS) of B. pseudomallei contributes to the formation of MGCs by translocating effector proteins into cells [16]. BipB, a known T3SS translocator protein, is also reported to mediate MGCs formation in infected macrophage [17]. MGCs has been reported to facilitate localized dissemination of B. pseudomallei [18], but the physiological function of host cell fusion induced by B. pseudomallei is still poorly understood.

The intracellular lifestyle of B. pseudomallei affected the biological functions of host cells. Currently, the identification of host cellular factors involved in the whole process of B. pseudomallei infection is limited. Whole-genome microarray studies can elucidate genes critical for bacterial survival, pathogenesis, intracellular life-cycle and virulence. This powerful technology has been employed in a murine macrophage model of acute melioidosis and innate immunity [19, 20]. Therefore, we used microarray analysis to investigate the global transcriptional response of A549 cells infected with B. pseudomallei at three key time points: 0 hpi (NC), 6 hpi (EI) and 12 hpi (LI) to better understand the associated differential expressed genes in the whole process of B. pseudomallei infection. Our data indicated that the DEGs of A549 cells responded to B. pseudomallei infection were mainly related to inflammation and stress response.

2 Results

2.1 B. pseudomallei promotes the formation of MGCs

To observe the cell morphology, cytoskeleton protein actin stained with Actin-Tracker Green, and confocal microscope was emploied. A time series assessment of A549 cell phenotype infected with B. pseudomallei was shown in Fig. 1. Three replicates were carried out in each group. No microreactive lesions were observed at 0 hours post inoculation (hpi). By 6 hpi, the occurrence rate of MGCs was 3.64 ± 0.79%, most of the infected cells didn’t fuse in this stage, maintaining normal cell morphology with clear cell boundary and intact outline. However, at 12 hpi, the MGCs had developed much larger and the rate increased up to 43.69 ± 8.65% (Fig. 1A). There was a significant difference in the percentage of MGCs formation between 6 hpi and 12 hpi ($t = 4$, $P = 0.001$), as seen in Fig. 1B. According to the formation of MGCs compared to control cells (0 hpi), we designated the interval between 0 hpi and 6 hpi as early infected stage (EI) and the interval between 6 hpi to 12 hpi as late infected stage (LI). Specially, filamentous actin tail of B. pseudomallei for directional movement within A549 cytosol were also found

as shown by the white arrow in the Fig. 1A, and mass replication of B. pseudomallei could be seen in every mature MGC.

2.2 Microarray data analyses of early and late infected stages

We analyzed total mRNA in different infected stages (EI, and LI) using the microarray analyses. Compared with NC, we observed a set of 325 differentially expressed genes (95 genes↑and 230 genes↓) in EI (Table S1) and 103 differentially expressed genes (44 genes↑and 59 genes↓) in LI (Table S2) on the mRNA level with the foldchange ≥ 1.5 and a P-value < 0.05. Thirty-five common genes showed a significant difference were found in the both infected stages, as seen in Fig. 2A. Their expression profile was listed in Table 2, as shown in Fig. 2B. The relative mRNA expression of the selected genes were confirmed by RT-qPCR, and the results showed ANXA9, BCL2, CLDN7 and IL1A reduced 0.56- (0.29-), 0.28- (0.71-), 0.75- (0.31-), and 0.83- (0.76-) fold, on the other hand, ATF4, GKN2, ICAM1, IL6, NFκB2 and TNFAIP3 increased 1.22- (1.59-), 1.41- (1.58-),4.05- (2.70-), 1.95- (1.87-), 1.54- (1.54-), and 1.55- (2.38-) fold, respectively, in EI and LI compared with NC (Fig. 2C), numbers in brackets represented foldchange of verified genes in LI. The RT-qPCR results were consistent with our microarray results.

Table 1

Primer sequences for analysis of gene expression using qRT-PCR

Primer name	Sequence (5' → 3')	Product size (bp)
ANXA9-F	TTCAGCGTGGACAAGGAT	171
ANXA9-R	TGCCTGTAGAGACTTCATCA	
ATF4-F	CCTTCACCTTCTTACAACCTCTTCC	125
ATF4-R	GTAGTCTGGCTTCCTATCTCCTTCA	
BCL2-F	ATCCGACCACTAATTGCCAAG	123
BCL2-R	TTCCATCCGTCTGCTCTTCA	
CLDN7-F	TCATCGTGGCAGGTCTTG	186
CLDN7-R	CAGGACAGGAACAGGAGAG	
GKN2-F	ACTTACTCCAGCACCTTCCTCTC	148
GKN2-R	GTCTCCTGAACATTGCCACCATT	
ICAM1-F	TATGGCAACGACTCCTTCTC	111
ICAM1-R	TGTCTCCTGGCTCTGGTT	
IL1A-F	TAGTGAGACCAACCTCCTCTTCT	189
IL1A-R	AGACAAGTGAGACTCCAGACCTA	
IL6-F	GTGAGGAACAAGCCAGAG	181
IL6-R	CGCAGAATGAGATGAGTTG	
NFκB2-F	AGGACGAGAACGGAGACA	125
NFκB2-R	GTGGTTGGTGAGGTTGACA	
TNFAIP3-F	GTTCCTCCTCTCCTACCAAG	108
TNFAIP3-R	ACGATGAAGCAGTCCTGAT	
GAPDH-F	ACAACTTTGGTATCGTGGAAGG	101
GAPDH-R	GCCATCACGCCACAGTTTC	

Table 2

Differentially expressed genes of A549 infected with Burkholderia pseudomallei during Early (6 hpi) and Late (12 hpi) infected stages in contrast to control cells (EI/LI).

Gene	Functional category and Protein name	mRNA Accession	Fold Change (EI / LI)
Regulation of immune system process			
SPINK5	Serine protease inhibitor Kazal-type 5	NM_001127698	0.31/0.56
MAP2K6	Dual specificity mitogen-activated protein kinase kinase 6	NM_002758	0.33/0.54
IL20RB	Interleukin-20 receptor subunit beta	NM_144717	0.54/0.62
THBS1	Thrombospondin-1	NM_003246	2.19/1.86
TNFAIP3	Tumor necrosis factor alpha-induced protein 3	NM_006290	2.70/2.90
IL6	Interleukin-6	NM_000600	2.72/2.19
IL1A	Interleukin-1 alpha	NM_000575	0.55/0.44
ALOX5AP	Arachidonate 5-lipoxygenase-activating protein	NM_001629	0.45/0.64
ATF4	Cyclic AMP-dependent transcription factor ATF-4	NM_001675	1.57/1.66
GKN2	Gastrokine-2	NM_182536	2.12/2.51
EIF2AK4	eIF-2-alpha kinase GCN2	NM_001013703	1.58/1.83
F3	Tissue factor	NM_001993	2.00/1.73
NFκB2	Nuclear factor NF-kappa-B p100 subunit	NM_001077494	1.68/1.78
Cell-cell adhesion			
ANXA9	Annexin A9	NM_003568	0.57/0.37
CLDN7	Claudin-7	NM_001307	0.60/0.48
ICAM1	Intercellular adhesion molecule 1	NM_000201	1.97/1.64
UBASH3B	Ubiquitin-associated and SH3 domain-containing protein B	NM_032873	2.34/2.12
SAMD9L	Sterile alpha motif domain-containing protein 9-like	NM_152703	0.55/0.43
CTGF	Connective tissue growth factor	NM_001901	2.06/1.85
Apoptotic process			

Gene	Functional category and Protein name	mRNA Accession	Fold Change (EI / LI)
GADD45A	Growth arrest and DNA damage-inducible protein GADD45 alpha	NM_001924	2.06/1.79
FOSL1	Fos-related antigen	NM_005438	2.07/1.95
MT1X	Metallothionein-1X	NM_005952	2.39/2.55
BCL2	Apoptosis regulator Bcl-2	NM_000633	0.62/0.66
IGFBP3	Insulin-like growth factor-binding protein 3	NM_001013398	1.86/1.77
Regulation of transport			
RAB26	Ras-related protein Rab-26	NM_014353	0.54/0.64
ANKRD1	Ankyrin repeat domain-containing protein 1	NM_014391	2.56/2.49
STC2	Stanniocalcin-2	NM_003714	2.90/2.30
DENND2C	DENN domain-containing protein 2C	NM_198459	1.91/1.83
PLD1	Phospholipase D1	NM_002662	0.62/0.55
G protein-coupled receptor signaling pathway			
PPYR1	Neuropeptide Y receptor type 4	NM_005972	0.37/0.65
GPRIN3	G protein-regulated inducer of neurite outgrowth 3	NM_198281	0.39/0.65
Cytoskeletal protein binding			
EPB41L4A	Band 4.1-like protein 4A	NM_022140	0.39/0.54
Zinc ion binding			
MMP7	Matrilysin	NM_002423	2.22/1.76
CA11	Carbonic anhydrase-related protein 11	NM_001217	0.60/0.66
Methyltransferase activity			
METTL7A	Methyltransferase-like protein 7A	NM_014033	0.23/0.56

2.3 Bioinformatics analyses

The functions of 35 commom DEGs from both EI and LI in A549 cells upon B. pseudomallei infection was further classified by GO term (Fig. 3A). The annotation of biological processes (BP) cluster analysis indicated that most differentially regulated genes were mainly related to inflammation and stress response, including inflammatory response, cellular response to tumor necrosis factor, cellular response

to lipopolysaccharide, positive regulation of NF-κB transcription factor activity and positive regulation of ERK1 and ERK2 cascade, and apoptotic process. Cell component (CC) annotations indicated most genes with differential expression were distributed across a variety of cellular components, including membranes, endoplasmic reticulum and extracellular region. Molecular function (MF) annotations showed that A549 cells infected with B. pseudomallei most frequently underwent functional changes related to binding and transcriptional activator activity. The KEGG pathway analysis also indicated that the top ten KEGG enrichment pathways were mainly related to inflammation and stress response, such as TNF, Epstein-Barr virus infection, NF-kappa B, MAPK, HTLV-I infection, Apoptosis, JAK-STAT, PI3K-Akt, NOD-like receptor and Inflammatory bowel disease signaling pathways, ranking by p-value as shown in Fig. 3B, listed in Table S3.

2.4 Validation of DEGs in inflammation and stress response

MGCs are mainly formed by the fusion of somatic cell and considered as characteristic feature at chronic inflammatory sites [21]. Bioinformatic analyses also revealed the DEGs involved in inflammation and stress response. In the present study, the proteins of p-eIF2α, ATF4, NF-κB2 (p100/p52) were selected as transcriptional activator in inflammation and IL-1β was selected as it involved in the proinflammatory response, for western bloting analysis to verify this phenomenon, as shown in Fig. 4A. p-eIF2α (foldchange = 1.32, t = 4.402, p = 0.012), ATF4 (foldchange = 1.91, t = 9.519, p = 0.001) and p52 (fold change = 1.53, t = 7.061, p = 0.002) were significantly up-regulated in EI relative to NC. Similarly, the significantly up-regulation was also found in LI with p-eIF2α (fold change = 1.56, t = 7.828, p = 0.001), ATF4 (fold change = 2.53, t = 14.08, p < 0.001), and p52 (fold change = 2.32, t = 9.918, p = 0.001) (Fig. 4B). With B. pseudomallei infection prolonged, the expression level of IL-1β (fold change = 1.28, t = 4.726, p = 0.009) was significantly increased in LI. There was no significant change about the expression level of p100 in both EI and LI. This was consistent with our transcriptome results of microarray analyses (Table 2). The eIF2α/ATF4 axis and NF-κB2 pathway were activated in B. pseudomallei-infected A549 cells.

3 Discussion

B. pseudomallei epidemic area is reported to be expanding in tropical and subtropical countries worldwide [22], including the South China Sea and Taiwan Strait [23, 24], and has been listed as a Tier-1 (top tier) select agent [2]. The intracellular lifestyle of B. pseudomallei in host cells has been reported to impact the severity of melioidosis, ranging from acute fatal sepsis to chronic infection with or without clinical symptoms [21, 25, 26]. However, the information about how B. pseudomallei impact on host cell responses is still limited during the whole intracellular infection processare. In this study, B. pseudomallei infection of a human lung epithelial A549 cell model was used for the global transcriptomic responses at early infected stage and late infected stage in contrast to control cells. We found the differential expression genes mainly involved in inflammation and stress response.

The A549 cell line is known to be a highly susceptible to infection of B. pseudomallei [3, 12, 27], and researches about many other intracellular bacteria infection also used A549 cell model. In the current study, the transcriptomic kinetics following lastingness of A549 infected with B. pseudomallei was conducted by GeneChip Human Gene 2.0 ST Arrays from Affymetrix, which represents approximately 30,654 transcribed genes. Microarray technology for transcriptome yields a large amount of data, and it is important to validate differential expression by independent methods, which conformed to the results of microarray assay. Real-time quantitative PCR analysis of random ten DEGs, including IL-6 and TNF-α (Fig. 2C), were therefore conducted, although there were fold differences between the RT-qPCR and transcriptome data, the result indicated that the expression profiles of differentially expressed genes in A549 were notably changed with the infection of B. pseudomallei.

In general, innate immune mechanisms are critical in determining the outcome of infections caused by bacterial pathogens. Recent studies have reported that B. pseudomallei increased the production of inflammatory cytokines such as TNF-α, IL-1β and IL-6 in vivo in serum samples of melioidosis patients [28]. Proinflammatory cytokine mRNA of TNF-α, IL-1β and IL-6 increased in the liver of mice following infected with B. pseudomallei [29]. In agreement with previous studies, our results showed that B. pseudomallei elevated IL-1β level and increased the mRNA expression of TNFAIP3 and IL-6 in human lung epithelial cell A549. Several lines of evidence suggest that one major role of eIFα/ATF4 pathway is to mediate the induction of a gene expression program referred to as the integrate stress response (ISR) [30, 31], involved in amino acid deficiency, endoplasmic reticulum stress (ERS), oxidative stress and drug resistance [32–34]. Our team's previous research indicated that B. pseudomallei could enhance NF-κB pathway in RAW264.7 macrophage cell through down-regulating TRAF3, a well-known negative regulator of the NF-κB, via increasing miR-3473 [35]. We further validated the transcriptional activator in inflammation, including p-eIF2α, ATF4 and NF-κB2. The data yield that B. pseudomallei exposure could active the eIF2α/ATF4 pathway and NF-κB2. B. pseudomallei may adjust host inflammation and stress response to cope with the intracellular encountered stress.

Previous studies have reported B. pseudomallei can in fact induce cell fusion leading to MGCs formation in both phagocytic and nonphagocytic cell lines [12, 36]. Cell fusion and the formation of MGCs have long been regarded as a possible mechanism for B. pseudomallei to cell-to-cell spreading [21]. In the present study, we found B. pseudomallei could induce A549 cells fusion, resulting in the formation of MGCs at the late infected stage, and B. pseudomallei were massively replicated in MGCs, which was consistent with previous studies. Additionally, The formation of MGCs was also found to exist in many other intracellular infectious agents such as human immunodeficiency virus (HIV), cytomegalovirus (CMV) and herpes simplex virus (HSV) [37–39]. It is reported that persistent existence of mycobacterial species leads to the formation of MGCs which play important roles in many physiological and pathological processes [40]. Meanwhile, B. pseudomallei could form filamentous actin tail whether in the early or late stage of infection, as seen in the Fig. 1A. Studies have shown that actin-based motility is an essential prerequisite for the production of MGCs and the spread of B. pseudomallei from cell-to-cell [21]. And recent evidences indicate that actin-based motility of B. pseudomallei is dependent upon the autosecreted protein, BimA [41]. While it still remains unresolved whether MGC are beneficial to the host,

that is, by prevention of bacterial spread, or whether they promote B. pseudomallei persistence. In our study, the formation of MGCs induced by B. pseudomallei may be a characteristic feature at chronic inflammatory sites in A549 cells to escape from intracellular immune defense mechanisms or help B. pseudomallei accessed to nutrients to achieve replication.

4 Conclusions

Our study has elucidated the differential expression genes profiles of A549 cells infected by B. pseudomallei during early and late infected stages. We have also verified the DEGs with qRT-PCR and western bloting. Mass replication of B. pseudomallei have been seen in MGC. Our data indicated that differentially-expressed gens which identfied in the early and late infected stages play significant roles in inflammation and stress response. In conclusion, B. pseudomallei induced the formation of MGCs in A549 likely made the battle turn even more into accessing to nutrients and spreading from cell to cell through the filamentous actin tail to achieve the survival.

5 Methods

5.1 Cell lines and bacterial strains

A549 human lung epithelial cell line (ATCC, CCL_185) was cultured in DMEM medium (Gibco), containing 10% fetal bovine serum (FBS, Gibco) and without antibiotics, in a humidified atmosphere of 5% CO_2 at 37˚C. B. pseudomallei C006 strain (BPC006) was used for bacterial infection, which it was isolated from a melioidosis patient in Hainan, China, and had been completely sequenced [42]. BPC006 was cultured in Luria-Bertani (LB) broth at 37 °C with shaking at 200 rpm. After overnight culture (~ 13 h), the concentration of BPC006 were measured by means of the optical density at 600 nm (OD_{600}). The experiment that manipulated B. pseudomallei was performed in biosafety level three (BSL-3) laboratory conditions.

5.2 Infection, Confocal microscopy and MGCs formation

Bacterial invasion of A549 cells followed our previously described strategy [10], with minor modifications. A549 cells were diluted to 1.5×10^5/mL, and 1 mL cell suspension was plated in each well of a 12-well plate containing glass coverslips (NEXT, China). Cells were co-incubated with B. pseudomallei at the indicated multiplicity of infection of 10 (MOI = 10) for 2 h, then washed twice with PBS (Beyotime, Shanghai, China). Subsequently, Cells were continued to grow in fresh culture supplemented with 250 μg/mL kanamycin (TIANGEN, Beijing, China) to kill the extracellular bacteria.

For confocal microscopy, cells were fixed at 6 hpi or 12 hpi in 4% paraformaldehyde (PFA, Electron Microscopy Sciences), then washed extensively with PBS buffer, and permeabilized with 0.3% Triton X-100 for 10 min. Coverslips were then incubated with rabbit anti-B. pseudomallei serum (1:200) at 4˚C overnight. Subsequently, overslips were incubated with the Alexa Fluor 568 anti-rabbit secondary antibody (1:2000, Molecular Probes, A-11036) at room temperature for 1 h. The cytoskeleton protein actin

was stained with Actin-Tracker Green (1:200, Beyotime, Shanghai, China). Nuclei was counterstained with DAPI (300 nM, Life technologies). Finally, coverslips were upsided down on the glass slide dripped with fluorescence mounting medium (Dako Cytomation). Images were obtained by a confocal microscopy (Zeiss, Germany).

MGC was counted as a cell containing at least three nuclei. The MGC formation efficiency was counted according to the method outlined in previous report [16]. In brief, MGC formation percentage was detected by a 20 × objective using the following formula:

$$\mathrm{MGCs'percentage} = \frac{\text{Nucleis in MGCs}}{\text{Total nucleis}} \times 100\%.$$

A minimum of 2,300 nucleis were counted for each condition and three replicates were used at each time point in the test.

5.3 GeneChip ™ microarray assay

Total RNA from the three groups were extracted by means of TRIzol reagent (Invitrogen, Carlsbad, CA, USA). The Affymetrix Whole Transcript Expression array procedure was performed according to manufacturer's protocol of GeneChip Human Gene 2.0 ST Arrays. In brief, the cDNA was synthesized using the Affymetrix GeneChip®Whole Transcript (WT) cDNA Synthesis and Amplification Kit. The sense cDNA was then fragmented and labelled with biotin using Affymetrix WT Terminal Labelling Kit. The labeled DNA target (~ 2.3 μg) were hybridized on the Affymetrix Gene Chip Human 2.0 ST Arrays for 16 h at 45 °C. The hybridized Affymetrix Gene Chip Human 2.0 ST arrays were then washed and stained using the Affymetrix Wash & Stain Kit, and scanned with an Affymetrix GeneChip® Scanner 3000-7G. Signal values were verified by Affymetrix® GeneChip™ Command Console software. Probe sets with a cut-off level of 1.5-fold change and a p-value lower than 0.05 were considered as significantly regulated.

5.4 Validation of microarray data

To validate the data generated from GeneChip™ microarray assay, 10 DEGs were randomly selected for RT-qPCR analysis. In brief, the total RNA was extracted by TRIzol (Invitrogen, Carlsbad, CA, USA). Next, cDNA was retro-transcribed from 1 μg of the template RNA using PrimeScript™ RT reagent Kit with gDNA Eraser (Takara, Dalian, China). Then SYBR Green PCR Kit (Takara Biotechnology Co., Ltd., Dalian, China) was used for RT-qPCR, CFX96 Touch Real-Time PCR detection system (Bio-Rad, USA) was used for fluorescence signal detection. The conditions for qPCR were 95 °C for 2 min, then 95 °C for 5 s and 60 °C for 30 s, for a total of 39 cycles. Three replicates were conducted. The relative expression levels of mRNAs were calculated by the method of $2^{-\Delta\Delta CT}$.

5.5 Bioinformatics annotation and cluster analysis

Gene Ontology (GO) analysis is a functional annotation method that commonly used for large-scale transcriptomic data. DEGs from EI and LI were uploaded into Annotation Visualization and Integrated Discovery (DAVID, http://david.ncifcrf.gov) for annotation and visual analysis. KEGG Orthology-Based

Annotation System (KOBAS, http://kobas.cbi.pku.edu.cn/home.do) was performed for top ten pathway enrichment analysis of identified DEGs. Terms with a P-value < 0.05 and an FDR of ≤ 0.05 were considered statistically significant.

5.6 Western blot analysis

Cell lysates were obtained from the groups of NC, EI and LI. BCA Protein Assay (Beyotime, Beijing, China) was used for protein concentration determination. The samples 40 μg in each group were loaded on 10% SDS-PAGE, and then were transferred to PVDF membranes (Roche, Switzerland). Membranes blocked with 5% (w/v) skimmed milk was subsequently executed at room temperature (RT) for 2 h, followed by an overnight incubation at 4 °C with the primary antibody of IL-1β (CST 12703, 1:1000) or Phospho-eIF2α (CST 3398, 1:1000) or ATF4(CST 11815, 1:1000) or NF-κB2 p100/p52 (CST 4882, 1:1000). Membranes were subsequently incubated with appropriate secondary antibody at RT for 1.5 h. The signals were detected with ECL detection reagents using an electrogenerated chemiluminescence detection system (ChemiDoc XRS System, Bio-Rad, USA), and the density of each protein band was quantified using Image Lab softwar 6.0 (Bio-Rad Laboratories). GAPDH (CST 8884, 1:1000) and β-actin (CST 3700, 1:5000) was used as loading control and all experiments were performed three times.

5.7 Statistical analysis

SPSS 23.0 statistical package for Windows (SPSS, Chicago, IL, USA) was used for statistical analysis. Data was expressed as the mean ± standard deviation (SD) from three independent experiments. Statistical significance was defined as P-value being lower than 0.05.

Abbreviations

MGCs: Multinucleated Giant Cells; EI: Early Infected stage; LI: Late Infected stage; RT-qPCR: Real-Time quantitative PCR; IL-1A: Interleukin-1A; IL-6: Interleukin-6; TNF-α: Tumor Necrosis Factor-alpha; p-eIF2α: Phosphorylation of the Alpha Subunit of Eukaryotic Initiation Factor 2; ATF4: Cyclic AMP-dependent transcription factor 4; NF-κB2: Transcription Factor p52; BPC006: *B. pseudomallei* C006 strain; DEG: Differential Expression Gene; GO: Gene Ontology; KEGG: Kyoto Encyclopedia of Genes and Genomes; WHO: World Health Organization.

Declarations

Ethics approval and consent to participate

Not applicable.

Consent for publication

Not applicable.

Availability of data and materials

All data generated or analyzed during this study are publicly available and included in this published article.

Competing interests

The authors declare that they have no competing interests

Funding

This work was supported by the National Natural Science Foundation of China (NSFC, Grant No. 31970135 and 81971907) and Third Military Medical University Science Foundation of Outstanding Youth (2017YQRC-07).

Authors' contributions

CLR was fully responsible for the study, including study design, data collection, data analysis and writing. CM and YPX worked with CLR to complete all experiments, and manuscript correction. The work of MJZ, ZQH and SQY were mainly about cells and bacterial culture. YZ and JMY worked together to help experimental material management. LD was fully responsible for research funding management and reimbursement. XHM and QL bore the fund. YLL reviewed the design of this article and got in touch with the research materials. All authors read and approved the final manuscript.

Acknowledgments

We thank Gminix (Shanghai, China) for its assistance with the GeneChip™ microarray assay.

Author details

1. Department of Clinical Microbiology and Immunology, College of Pharmacy and Medical Laboratory, Army Medical University (Third Military Medical University), Chongqing, China; 2.
Department of Pharmacy, The Second Affiliated Hospital, Army Medical University (Third Military Medical University), Chongqing, China.

References

1. Wiersinga WJ, Currie BJ, Peacock SJ: **Melioidosis**. *The New England journal of medicine* 2012, **367**(11):1035-1044.
2. Wiersinga WJ, van der Poll T, White NJ, Day NP, Peacock SJ: **Melioidosis: insights into the pathogenicity of *Burkholderia pseudomallei***. *Nature reviews Microbiology* 2006, **4**(4):272-282.
3. Limmathurotsakul D, Golding N, Dance DA: **Predicted global distribution of *Burkholderia pseudomallei* and burden of melioidosis**. 2016, **1**:15008.
4. Wiersinga WJ, Virk HS, Torres AG, Currie BJ, Peacock SJ, Dance DAB, Limmathurotsakul D: **Melioidosis**. *Nature reviews Disease primers* 2018, **4**:17107.

5. Titball RW, Burtnick MN, Bancroft GJ, Brett P: ***Burkholderia pseudomallei*** **and Burkholderia mallei vaccines: Are we close to clinical trials?** *Vaccine* 2017, **35**(44):5981-5989.
6. Zueter A, Yean CY, Abumarzouq M, Rahman ZA, Deris ZZ, Harun A: **The epidemiology and clinical spectrum of melioidosis in a teaching hospital in a North-Eastern state of Malaysia: a fifteen-year review**. *BMC infectious diseases* 2016, **16**:333.
7. Stevens MP, Friebel A, Taylor LA, Wood MW, Brown PJ, Hardt WD, Galyov EE: **A *Burkholderia pseudomallei* type III secreted protein, BopE, facilitates bacterial invasion of epithelial cells and exhibits guanine nucleotide exchange factor activity**. *Journal of bacteriology* 2003, **185**(16):4992-4996.
8. Gong L, Cullinane M, Treerat P, Ramm G, Prescott M, Adler B, Boyce JD, Devenish RJ: **The *Burkholderia pseudomallei* type III secretion system and BopA are required for evasion of LC3-associated phagocytosis**. *PloS one* 2011, **6**(3):e17852.
9. Srinon V, Chaiwattanarungruengpaisan S, Korbsrisate S, Stevens JM: ***Burkholderia pseudomallei*** **BimC Is Required for Actin-Based Motility, Intracellular Survival, and Virulence**. *Frontiers in cellular and infection microbiology* 2019, **9**:63.
10. Li Q, Fang Y, Zhu P, Ren CY, Chen H, Gu J, Jia YP, Wang K, Tong WD, Zhang WJ *et al*: ***Burkholderia pseudomallei*** **survival in lung epithelial cells benefits from miRNA-mediated suppression of ATG10**. *Autophagy* 2015, **11**(8):1293-1307.
11. Hu ZQ, Rao CL, Tang ML, Zhang Y, Lu XX, Chen JG, Mao C, Deng L, Li Q, Mao XH: **Rab32 GTPase, as a direct target of miR-30b/c, controls the intracellular survival of *Burkholderia pseudomallei* by regulating phagosome maturation**. *PLoS pathogens* 2019, **15**(6):e1007879.
12. Kespichayawattana W, Rattanachetkul S, Wanun T, Utaisincharoen P, Sirisinha S: ***Burkholderia pseudomallei*** **induces cell fusion and actin-associated membrane protrusion: a possible mechanism for cell-to-cell spreading**. *Infection and immunity* 2000, **68**(9):5377-5384.
13. McNally AK, Anderson JM: **Macrophage fusion and multinucleated giant cells of inflammation**. *Advances in experimental medicine and biology* 2011, **713**:97-111.
14. Conejero L, Patel N, de Reynal M, Oberdorf S, Prior J, Felgner PL, Titball RW, Salguero FJ, Bancroft GJ: **Low-dose exposure of C57BL/6 mice to *burkholderia pseudomallei* mimics chronic human melioidosis**. *The American journal of pathology* 2011, **179**(1):270-280.
15. Wong KT, Puthucheary SD, Vadivelu J: **The histopathology of human melioidosis**. *Histopathology* 1995, **26**(1):51-55.
16. Whiteley L, Meffert T, Haug M, Weidenmaier C: **Entry, Intracellular Survival, and Multinucleated-Giant-Cell-Forming Activity of *Burkholderia pseudomallei* in Human Primary Phagocytic and Nonphagocytic Cells**. 2017, **85**(10).
17. Suparak S, Kespichayawattana W, Haque A, Easton A, Damnin S, Lertmemongkolchai G, Bancroft GJ, Korbsrisate S: **Multinucleated Giant Cell Formation and Apoptosis in Infected Host Cells Is Mediated by *Burkholderia pseudomallei* Type III Secretion Protein BipB**. *Journal of bacteriology* 2005, **187**(18):6556-6560.

18. Kespichayawattana W, Rattanachetkul S, Wanun T, Utaisincharoen P, Sirisinha S: ***Burkholderia pseudomallei*** **Induces Cell Fusion and Actin-Associated Membrane Protrusion: a Possible Mechanism for Cell-to-Cell Spreading**. *Infection and immunity* 2000, **68**(9):5377-5384.
19. Chin CY, Monack DM, Nathan S: **Genome wide transcriptome profiling of a murine acute melioidosis model reveals new insights into how *Burkholderia pseudomallei* overcomes host innate immunity**. *BMC genomics* 2010, **11**:672.
20. Tuanyok A, Tom M, Dunbar J, Woods DE: **Genome-wide expression analysis of *Burkholderia pseudomallei* infection in a hamster model of acute melioidosis**. *Infection and immunity* 2006, **74**(10):5465-5476.
21. Allwood EM, Devenish RJ, Prescott M, Adler B, Boyce JD: **Strategies for Intracellular Survival of *Burkholderia pseudomallei***. *Frontiers in microbiology* 2011, **2**:170.
22. Perumal Samy R, Stiles BG, Sethi G, Lim LHK: **Melioidosis: Clinical impact and public health threat in the tropics**. *PLoS neglected tropical diseases* 2017, **11**(5):e0004738.
23. Rao C, Hu Z, Chen J, Tang M, Chen H, Lu X, Cao L, Deng L, Mao X, Li Q: **Molecular epidemiology and antibiotic resistance of *Burkholderia pseudomallei* isolates from Hainan, China: A STROBE compliant observational study**. *Medicine* 2019, **98**(9):e14461.
24. Yang S: **Melioidosis research in China**. *Acta tropica* 2000, **77**(2):157-165.
25. Lazar Adler NR, Govan B, Cullinane M, Harper M, Adler B, Boyce JD: **The molecular and cellular basis of pathogenesis in melioidosis: how does *Burkholderia pseudomallei* cause disease?** *FEMS microbiology reviews* 2009, **33**(6):1079-1099.
26. Pilatz S, Breitbach K, Hein N, Fehlhaber B, Schulze J, Brenneke B, Eberl L, Steinmetz I: **Identification of *Burkholderia pseudomallei* genes required for the intracellular life cycle and in vivo virulence**. *Infection and immunity* 2006, **74**(6):3576-3586.
27. Kespichayawattana W, Intachote P, Utaisincharoen P, Sirisinha S: **Virulent *Burkholderia pseudomallei* is more efficient than avirulent Burkholderia thailandensis in invasion of and adherence to cultured human epithelial cells**. *Microbial pathogenesis* 2004, **36**(5):287-292.
28. Koosakulnirand S, Phokrai P, Jenjaroen K, Roberts RA, Utaisincharoen P, Dunachie SJ: **Immune response to recombinant *Burkholderia pseudomallei* FliC**. 2018, **13**(6):e0198906.
29. Ulett GC, Ketheesan N, Hirst RG: **Cytokine gene expression in innately susceptible BALB/c mice and relatively resistant C57BL/6 mice during infection with virulent *Burkholderia pseudomallei***. *Infection and immunity* 2000, **68**(4):2034-2042.
30. Abdel-Nour M, Carneiro LAM: **The heme-regulated inhibitor is a cytosolic sensor of protein misfolding that controls innate immune signaling**. 2019, **365**(6448).
31. B'Chir W, Maurin AC, Carraro V, Averous J, Jousse C, Muranishi Y, Parry L, Stepien G, Fafournoux P, Bruhat A: **The eIF2alpha/ATF4 pathway is essential for stress-induced autophagy gene expression**. *Nucleic acids research* 2013, **41**(16):7683-7699.
32. Zhang P, McGrath BC, Reinert J, Olsen DS, Lei L, Gill S, Wek SA, Vattem KM, Wek RC, Kimball SR *et al*: **The GCN2 eIF2alpha kinase is required for adaptation to amino acid deprivation in mice**. *Molecular*

and cellular biology 2002, **22**(19):6681-6688.

33. Harding HP, Zhang Y, Ron D: **Protein translation and folding are coupled by an endoplasmic-reticulum-resident kinase**. *Nature* 1999, **397**(6716):271-274.
34. Yerlikaya A, Kimball SR, Stanley BA: **Phosphorylation of eIF2alpha in response to 26S proteasome inhibition is mediated by the haem-regulated inhibitor (HRI) kinase**. *The Biochemical journal* 2008, **412**(3):579-588.
35. Fang Y, Chen H, Hu Y, Li Q, Hu Z, Ma T, Mao X: ***Burkholderia pseudomallei*-derived miR-3473 enhances NF-κB via targeting TRAF3 and is associated with different inflammatory responses compared to Burkholderia thailandensis in murine macrophages**. *BMC microbiology* 2016, **16**(1):283-283.
36. Harley VS, Dance DA, Drasar BS, Tovey G: **Effects of *Burkholderia pseudomallei* and other Burkholderia species on eukaryotic cells in tissue culture**. *Microbios* 1998, **96**(384):71-93.
37. Ciborowski P, Gendelman HE: **Human immunodeficiency virus-mononuclear phagocyte interactions: emerging avenues of biomarker discovery, modes of viral persistence and disease pathogenesis**. *Current HIV research* 2006, **4**(3):279-291.
38. Kinzler ER, Compton T: **Characterization of human cytomegalovirus glycoprotein-induced cell-cell fusion**. *Journal of virology* 2005, **79**(12):7827-7837.
39. Cole NL, Grose C: **Membrane fusion mediated by herpesvirus glycoproteins: the paradigm of varicella-zoster virus**. *Reviews in medical virology* 2003, **13**(4):207-222.
40. Gharun K, Senges J, Seidl M, Losslein A, Kolter J, Lohrmann F, Fliegauf M, Elgizouli M, Alber M, Vavra M *et al*: **Mycobacteria exploit nitric oxide-induced transformation of macrophages into permissive giant cells**. 2017, **18**(12):2144-2159.
41. Stevens MP, Stevens JM, Jeng RL, Taylor LA, Wood MW, Hawes P, Monaghan P, Welch MD, Galyov EE: **Identification of a bacterial factor required for actin-based motility of *Burkholderia pseudomallei***. *Molecular microbiology* 2005, **56**(1):40-53.
42. Fang Y, Huang Y, Li Q, Chen H, Yao Z, Pan J, Gu J, Tang B, Wang HG, Yu B *et al*: **First genome sequence of a *Burkholderia pseudomallei* Isolate in China, strain BPC006, obtained from a melioidosis patient in Hainan**. *Journal of bacteriology* 2012, **194**(23):6604-6605.

Figures

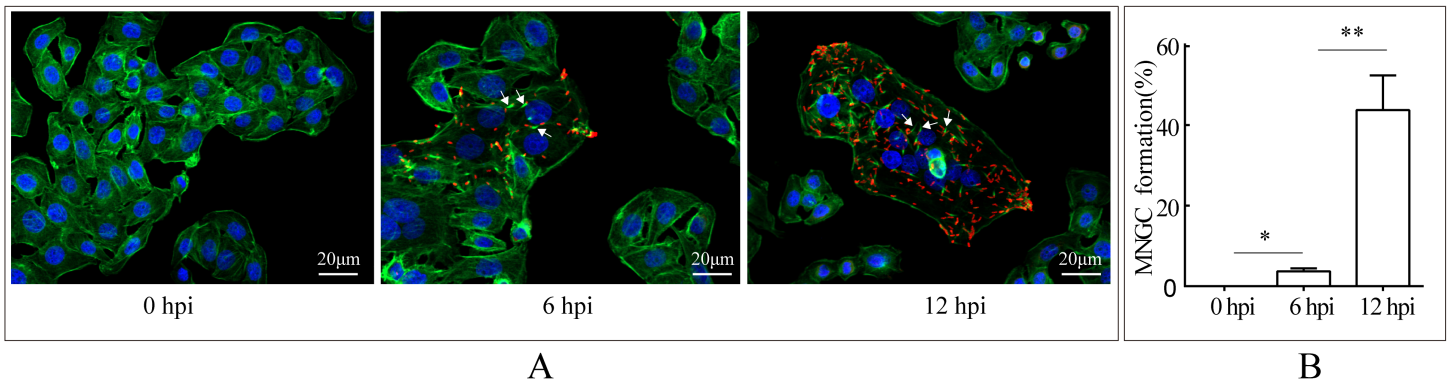

Figure 1

B. pseudomallei promotes MGCs formation A. Confocal microscope shown the formation of MGCs induced by B. pseudomallei at different infected times. Red is B. pseudomallei indicated by Alexa Fluor 568, Blue is nucleus indicated by DAPI, Green is cytoskeleton protein actin indicated by Actin-Tracker Green. The white arrow indicates filamentous actin tail of B. pseudomallei. B. The percentage of MGCs statisticed at different time points. Three replicates were used for each time point. Data are presented as mean ± SD, the asterisk indicates the significant difference (* $p < 0.05$, ** $p < 0.01$).

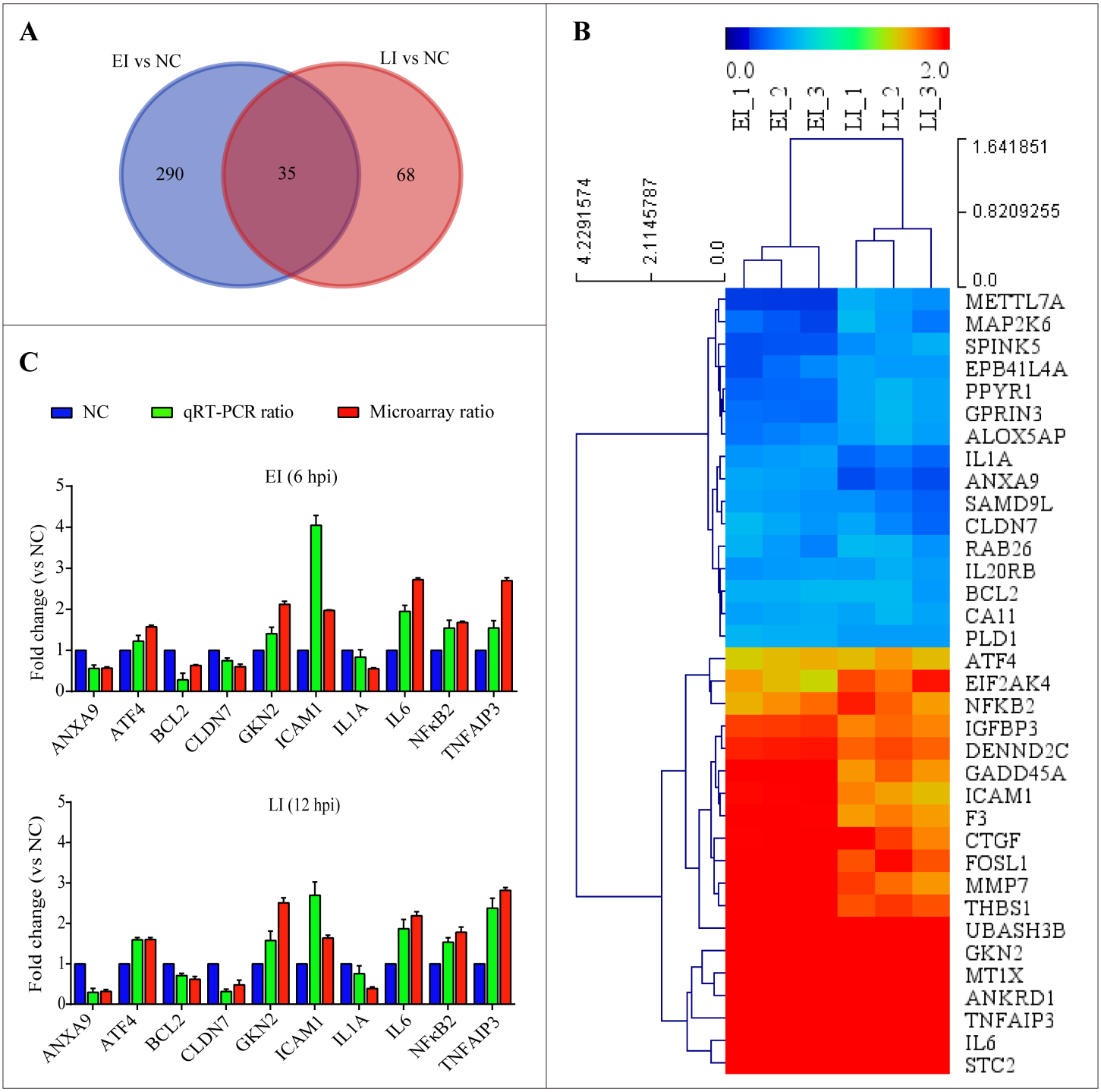

Figure 2

Differential expression genes (DEGs) between EI and LI. A. A set of 35 common DEGs in EI and LI on the mRNA level were observed. Cut-off level was 1.5-fold change, P-value < 0.05. B. Hierarchical clustering of common DEGs. Red: high expression levels; Blue: low expression level. C. RT-qPCR verified ten selected mRNAs in DEGs. The relative expression level of mRNA is expressed as a fold change relative to NC. Three replicates were used for each time point.

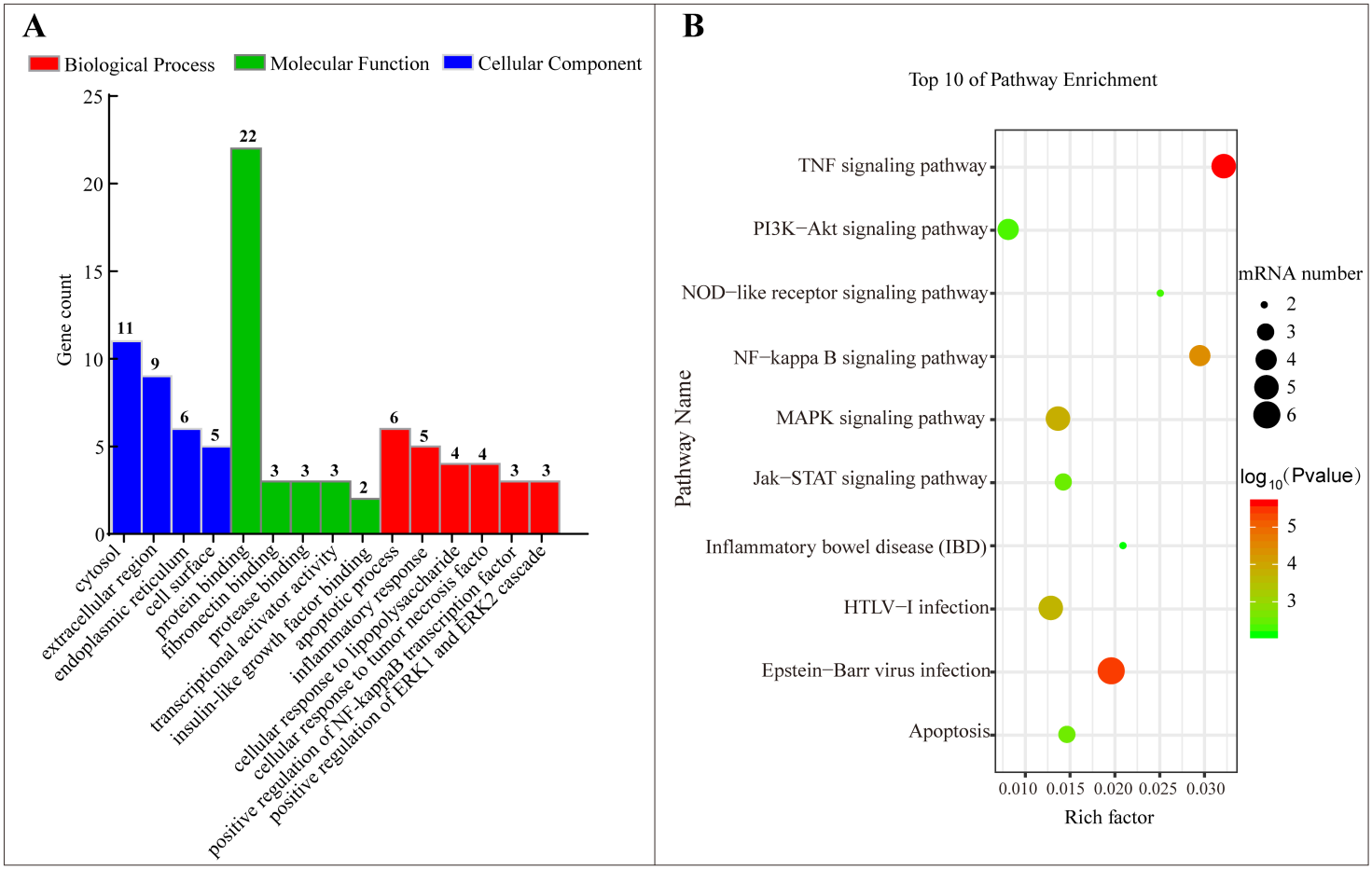

Figure 3

Gene ontology classification and KEGG analysis of DEGs. A. DEGs' gene ontology functional classification. The bar graph shows the distribution of DEGs in the terms of BP, CC and MF. B. Pathway enrichment analysis of DEGs. The Y-axis shows top ten enrichment pathways of DEGs, and the X-axis shows a rich factor. Rich factor=(The number of target genes in π path)/(All annotated genes in π pathway). π represents any one of the KEGG pathways. The higher the enrichment factor, the higher the degree of enrichment. The size of the dots indicates the number of target genes in the pathway, and the color of the dots reflects different P-value ranges.

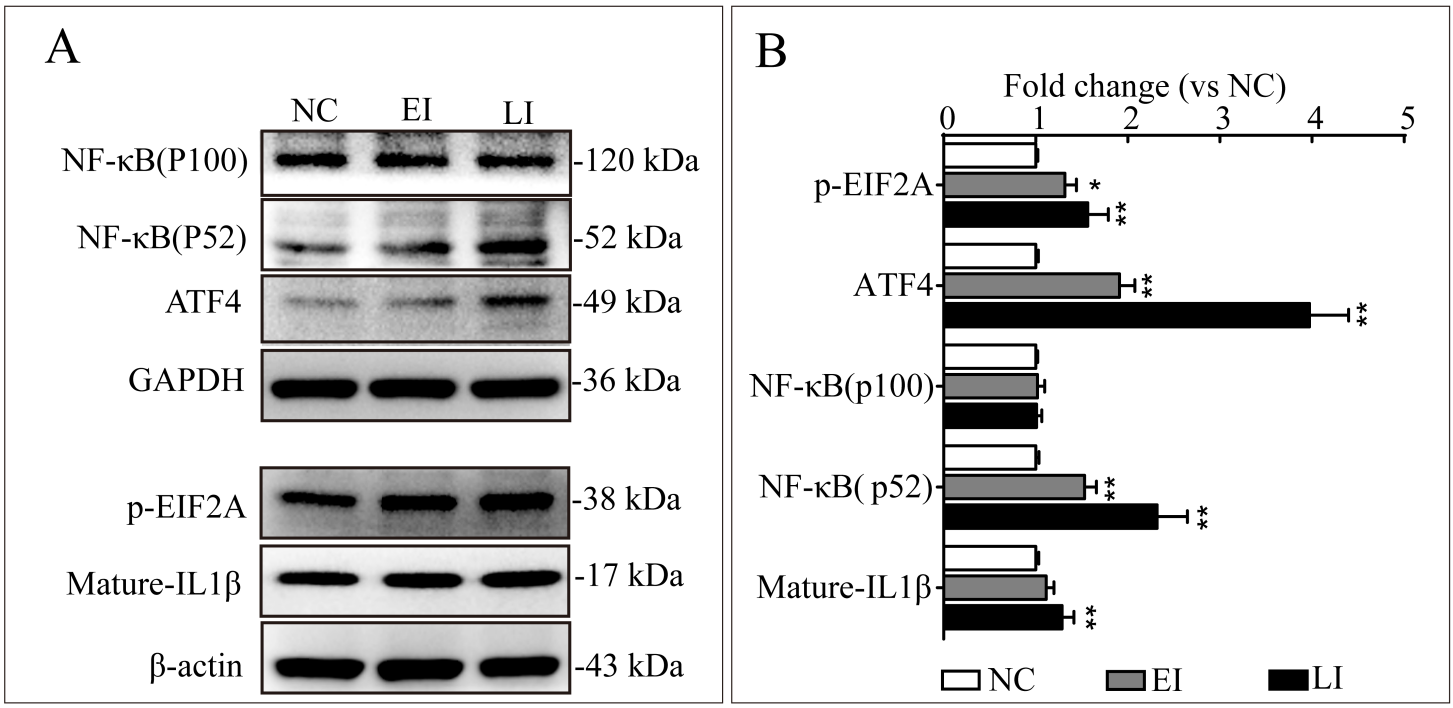

Figure 4

Western blot analysis of DEGs. Western blot analysis of DEGs involved in inflammation and stress responses. p-eIF2α, ATF4, NF-κB2 (p52/p100), and IL-1β were detected with their respective antibodies. GAPDH and β-actin was used as loading control and three replicates were performed, *p < 0.05, **p < 0.01.

Supplementary Files

This is a list of supplementary files associated with this preprint. Click to download.

- TableS1.xlsx
- TableS3.docx
- TableS2.xlsx